# Single-mode Er-doped fiber random laser with distributed Bragg grating feedback

**N. Lizárraga[1], N. P. Puente[2], E. I. Chaikina[*1], T. A. Leskova[3], and E. R. Méndez[1]**

[1]*División de Física Aplicada, Centro de Investigación Científica y de Educación Superior de Ensenada, Km. 107 carretera Tijuana-Ensenada, Ensenada, B. C., 22860, México*

[2]*Facultad de Ingeniería, Universidad Autónoma de Baja California, Apartado Postal 2732, Ensenada, México.*

[3]*Department of Physics and Astronomy and Institute for Surface and Interface Science, University of California, Irvine, CA 92697, USA*

*chaikina@cicese.mx*

**Abstract:** We report the implementation of a one-dimensional random laser based on an Er/Ge co-doped single-mode fiber with randomly spaced Bragg gratings. The random grating array forms a complex cavity with high quality factor resonances in the range of gain wavelengths centered around 1535.5 nm. The reflection spectra of the grating array and the emission spectra of the laser are investigated for different numbers of gratings. The experimental results are compared qualitatively with numerical simulations of the light propagation in one-dimensional Bragg grating arrays based on a transfer matrix method. The system is pumped at 980 nm and the experimentally observed output radiation presents a typical laser threshold behavior as a function of the pump power. We find that the laser output contains several competing spectral modes.



**OCIS codes:** (290.4210) Multiple scattering; (140.3510) Lasers, fibers

## References and links

1. H. Cao, "Lasing in random media," Waves in Random Media **13**, R1-R39 (2003).
2. M. A. Noginov, *Solid-State Random Lasers* (Springer, Berlin, 2005).
3. H. Cao, "Review on latest developments in random lasers with coherent feedback," J. Phys. A: Math. Gen. **38**, 10497-10535 (2005).
4. P. Sheng, *Introduction to Wave Scattering, Localization and Mesoscopic Phenomena* (Springer, Berlin, 2006).
5. X. Jiang and C. M. Soukoulis, "Theory and simulations of random lasers," in *Photonic Crystals and Light Localization in the 21st Century*, C. M. Soukoulis, ed. (Kluwer Academic Publishers, Dordrecht, The Netherlands, 2001), pp. 417-446.
6. A. L. Burin, M. A. Ratner, H. Cao, and R. P. H. Chang, "Random laser in one dimension," Phys. Rev. Lett **88**, 093904(1-4) (2002).
7. V. Milner and A. Genack, "Photon localization laser," Phys. Rev. Lett. **94**, 073901(4) (2005).
8. U. Frisch, C. Froeschle, J. -P. Scheidecker, and P. -L. Sulem, "Stochastic Resonance in One-Dimensional Random Media," Phys. Rev. A **8**, 1416-1422 (1973).
9. A. R. McGurn, K. T. Christensen, F. M. Mueller, and A. A. Maradudin, "Anderson localization in one-dimensional randomly disordered optical systems that are periodic on average," Phys. Rev. B **27**, 13120-13125 (1993).

#103290 - $15.00 USD Received 31 Oct 2008; revised 13 Dec 2008; accepted 13 Dec 2008; published 5 Jan 2009

10. M. V. Berry and S. Klein, "Transparent mirrors: rays, waves and localization," Eur. J. Phys. **18**, 222-228 (1997).
11. K. Yu. Bliokh, Yu. P Bliokh, and V. D. Freilikher, "Resonances in 1D disordered systems: localization of energy and resonant transmission, " J. Opt. Soc. Am. B**21**, 113-120 (2004).
12. P. Sebbah, B. Hu, J. M. Klosner, and A. Z. Genack, "Extended quasimodes within nominally localized random waveguides," Phys. Rev. Lett. **96**, 183902(4) (2006).
13. C. J. S. de Matos, L. de S. Menezes, A. M. Brito-Silva, M. A. Martinez- Gámez, A. S. L. Gomes, and C. B. de Araújo, "Random fiber laser," Phys. Rev. Lett. **99,** 153903(1-4) (2007).
14. S. Pissadakis, A. Ikiades, P. Hua, A. Sheridan, and J. Wilkinson, "Photosensitivity of ion-exchanged Er-doped phosphate glass using 248 nm excimer laser radiation," Opt. Express **12**, 3131-3136 (2004).
15. E. I. Chaikina, N. Lizárraga and E. R. Mendez, "Formation of the cavity in random Er-doped fiber laser ," Proc. of CLEO-IQEC-Europe-2007, SBN: 978-1-4244-0931-0.
16. O. Shapira and B. Fischer, "Localization of light in a random-grating array in a single-mode fiber," J. Opt. Soc. Am. B **22**, 2542-2552 (2005).
17. R. Kashyap, *Fiber Bragg Gratings* (Academic Press, San Diego, 1999).
18. G. A. Ball, W. W. Morey, and W. H. Glenn, "Standing-wave monomode erbium fiber laser," IEEE Phot. Technol. Lett. **3**, 613-615 (1991).
19. S.V. Chernikov, J. R. Taylor, and R. Kashyap, "Coupled-cavity erbium fiber lasers incorporating fiber grating reflectors," Opt.Lett. **18**, 2023-2025 (1993).
20. W. H. Loh and R. I. Laming, "1.55$\mu$m phase-shifted distributed feedback fibre laser," Electron. Lett. **31**, 1440-1442 (1995).
21. M. Sejka, P. Varming, J. Hübner, and M. Kristensen, "Distributed feedback $Er^{3+}$-doped fibre laser," Electron. Lett. **31**, 1445-1446 (1995).
22. A. Siegman, *Lasers* (University Science Books, Sausalito, 1986).
23. E. Desurvire, *Erbium-Doped Fiber Amplifiers, Principles and Applications* (Wiley InterScience, Inc., Hoboken, 2002).
24. J. B. Pendry, "Symmetry and transport of waves in one-dimensional disordered system," Adv. Phys. **43**, 461-542 (1994).
25. V. D. Freilikher and S. A. Gredeskul, "Localization of waves in media with one-dimensional disorder," in *Progress in Optics*, E. Wolf, ed. (North-Holland, Amsterdam, 1996), V. XXX, pp. 137-203.
26. K. Yu. Bliokh, Yu. P. Bliokh, V. Freilikher, A. Z. Genack, B. Hu, and P. Sebbah, "Localized Modes in Open One-Dimensional Dissipative Random Systems", Phys. Rev. Lett. **97**, 243904(4) (2005).

## 1. Introduction

Random lasers (RL), in which optical gain is combined with multiple scattering of the light inside an active medium, are the subject of scientific interest due to their unusual properties and promising potential applications [1, 2, 3]. In addition, lasing in random optical materials is closely related to another fundamental problem, namely, localization of light [4]. Random lasers have been experimentally demonstrated in different three-dimensional structures; among them are neodymium-glass powders, dye-$TiO_2$ solutions, ZnO nano-clusters, and $\pi$-conjugated polymer films [1]. One of the characteristic drawbacks of these 3D laser configurations is their inefficient pumping, which is directly associated with light scattering in the random medium.

One can expect that the properties of such lasers depend crucially on the dimensionality of the random laser medium - three-dimensional (3D), two-dimensional (2D), or one-dimensional (1D) - and a comparison of the dependence of their lasing properties with the dimensionality can help in the understanding of the nature of these lasers. There are several of theoretical publications on lasing in 1D random media [5, 6] but, as far as we know, there is only one experimental paper on lasing in a 1D random system [7]. In that work, microscopic glass slides were immersed in Rhodamin 6G dye or intermixed with chromophore-doped plastic sheets. The random nature of this 1D structure is associated with the natural fluctuations in the thicknesses of the slides and the inter-slide distances. One of the main features of this laser configuration is that both the pump and the emission longitudinal modes have localized cavities inside the structure. When these two light distributions overlap well, the pumping of the laser mode at this frequency is quite efficient, and a fairly low RL generation threshold is observed. Similar stack structures were also analyzed theoretically and investigated experimentally in relation with 1D light localization in Refs. [8, 9, 10, 11, 12]. It should be noticed that, under real experimental

#103290 - $15.00 USD Received 31 Oct 2008; revised 13 Dec 2008; accepted 13 Dec 2008; published 5 Jan 2009

conditions, such structures cannot be considered as strictly one-dimensional because of the inevitable misaligment of the slides and because of their optical imperfections.

A random fiber laser in which a suspension of rutile ($TiO_2$) particles in Rhodamine 6G solution is used to fill the hollow core of a photonic fiber was reported recently in Ref. [13]. The reduced dimensionality of the system, and the consequent concentration of the laser emission along the fiber axis, increased the efficiency of generation by at least two orders of magnitude in comparison with a similar system in bulk. The efficiency of the multimode laser emission (with up to several hundred transverse modes), would be expected to increase as the number of modes decreases.

In this paper we report experimental realization of the one-dimensional random fiber laser. Some preliminary results were presented in Ref. [15]. The laser system consists of an optically-pumped single-mode erbium-doped fiber (EDF) with an array of randomly distributed Bragg gratings (see Fig.1). A passive system, similar to the one used here, was investigated in Ref. [16] in connection with 1D light localization.

Rare-earth-doped fiber lasers have become quite common and there are several commercially available systems. Bragg fiber gratings [17], on the other hand, are also quite popular; they are used widely in telecommunication WDM systems, fiber optic sensors, and represent one of the most commonly used elements for the selection of the emission wavelength, and/or the reduction of the number of generated longitudinal modes in fiber optic lasers [18, 19]. These gratings can be considered as highly dispersive reflectors.

Distributed-feedback (DFB) configurations are also widely used in fiber lasers and semiconductor lasers with single-frequency operation. In the case of fiber lasers [20, 21], the distributed reflection occurs *via* regular fiber Bragg gratings recorded directly into the active part of the fiber, with typical lengths from a few millimeters to centimeters. Efficient pump absorption in such lasers can be achieved only for high dopant concentrations but, unfortunately, it is not easy to write Bragg gratings into fibers with such characteristics [14]. The result is that although this kind of single-frequency fiber laser is simple, compact, and robust, their output power is usually limited to some tens of milliwatts.

Unlike the stack system studied in [7], the fiber configuration under investigation here is essentially one dimensional. Indeed, the fiber supports only two guided modes at the operating wavelength $\lambda_s$, propagating in opposite directions inside the fiber, and the generated output light profile has, approximately, a Gaussian form. It is also important to mention that this cavity does not possess any resonance properties at the pump wavelength ($\lambda_p \approx 980$nm), i.e. the active medium can be pumped fairly uniformly and this can be done through one or both ends of the fiber.

In some ways, this configuration can be considered as a generalization of the above-mentioned distributed feedback fiber lasers that contains two uniform (and, in comparison, rather short) gratings recorded in the bulk of the doped fiber. The distributed laser cavity formed by a multitude of randomly spaced Bragg gratings increments the effective length of the cavity and, in this way, improves the efficiency of the system and the frequency selection.

## 2. Fabrication and characterization of an Er-doped fiber laser with randomly distributed Bragg gratings

The optical fiber used in the experiments is a commercial Er/Ge co-doped single mode optical fiber Er305 made by INO (International Optics Institute). The core diameter is $D_c \approx 6.1\,\mu$m, and the maximum absorption is about 8.2 dB/m at 1534 nm. Bragg gratings were recorded in the fiber core by exposing to the UV light from an intracavity frequency doubled Argon-ion laser ($\lambda_r = 244$nm) using a conventional mask technique [17]. The 10 mm-long mask has a spatial period of 1059.8 nm. The length of each one of the fabricated gratings $L_g$ was about

#103290 - $15.00 USD Received 31 Oct 2008; revised 13 Dec 2008; accepted 13 Dec 2008; published 5 Jan 2009

5 mm, and the distances $L_i$ between two neighboring gratings were randomly distributed in the range $4.2-5.8$ mm (see inset of Fig. 1). The total length of the structure was $L \approx N(L_g + L_i)$, where the largest number of gratings $N$ reached 31 in our experiments.

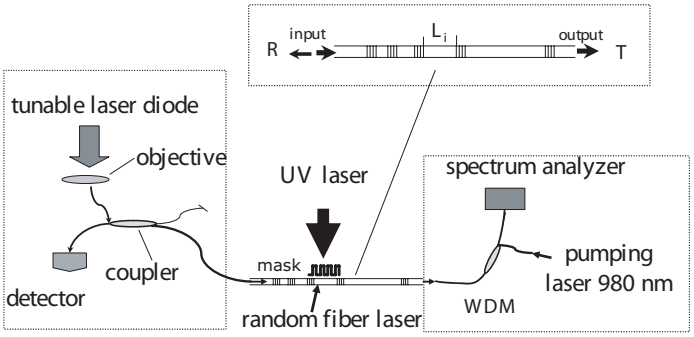


Fig. 1. Schematic diagram of the experimental setup.

Measurements of the gratings transmission/reflection coefficients with a spectral resolution of 0.001 nm were carried out in the spectral range $1520-1580$ nm, using a tunable semiconductor laser (New Focus Velocity-6300) with a coherence length of a few meters. Typically, a single fabricated grating had a narrow reflection spectrum centered on the average Bragg wavelength $\lambda_B \approx 1535.5$ nm, with a full width at half maximum (FWHM) $\Delta\lambda_g$ of about 0.17nm. Due to the inevitable variations in some experimental parameters, like recording exposure, alignment of the mask, and fiber tension during exposure, some dispersion in the central Bragg wavelength were observed, with a maximum deviation of about 0.27 nm. The typical reflectivity of one single grating was between 7 and 8%. Examples of the reflection spectra of the recorded random arrays of seven, fourteen, twenty and thirty one gratings are presented in Fig. 2. For the sake of

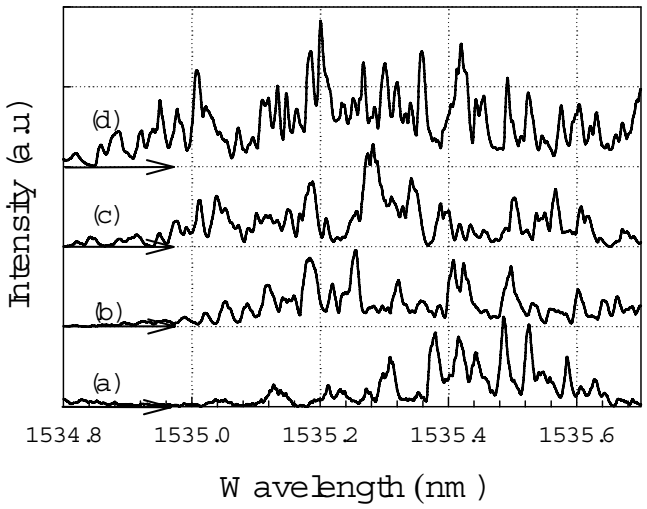


Fig. 2. Reflection spectra of arrays of (a) seven, (b) fourteen, (c) twenty, and (d) thirty one gratings. For clarity, the plots have been shifted vertically.

#103290 - $15.00 USD Received 31 Oct 2008; revised 13 Dec 2008; accepted 13 Dec 2008; published 5 Jan 2009

clarity the plots have been shifted vertically; the arrows under each curve denote the position of zero reflectivity for that curve. The spectra contain peaks whose positions change and acquire finer details as the number of gratings $N$ is increased.

The investigated fiber laser consisted of a 150 cm-long piece of Er/Ge co-doped fiber with an array of randomly spaced Bragg gratings recorded into it. In the experimental setup depicted in Fig. 1, the fact that there are three main parts of the arrangement has been emphasized. One part, shown on the left of the figure, represents the arrangement used to measure the reflection spectrum of the grating array during the fabrication process. The central part of the figure illustrates the sample and the arrangement used to fabricate the gratings. The other part, shown on the right of the figure, is related to the laser itself and contains the optical pump and the spectrophotometer used for the analysis of the laser emission spectrum.

Figure 3 shows spectra of the output emission of a RL with a cavity formed by 7 gratings, measured at different levels of relatively low pump intensities. The photoluminescence spectra shown in the two lower curves (black and red) correspond to situations below the laser threshold [22], and were obtained with pump powers of 7.0 and 7.5 mW. The upper curve (blue) corresponds to a situation slightly above threshold and was obtained with a pump power of 10 mW. A narrow lasing line at approximately 1535.5 nm can be observed for this case. It is pertinent to mention that the photoluminescence spectra of the Er/Ge co-doped fibers differ from those of a silica fiber doped only with Er [23].

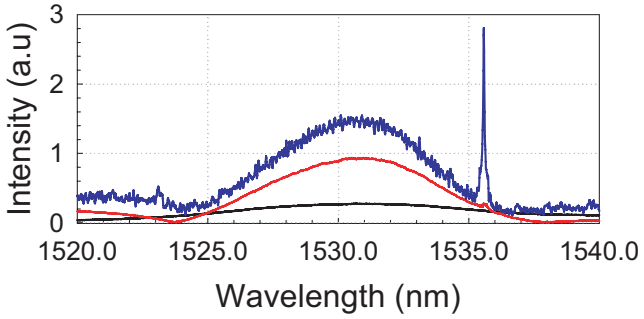


Fig. 3. Emission spectra of RL with 7 gratings measured at different pump levels: below (black and red curves) and above (blue curve) threshold.

In Fig. 4 we present measurements of the emission spectra of the RL with cavities containing 7, 14, 20, and 31 randomly distributed Bragg gratings (RDBG) for two values of the pump power; 20 mW for the red curves and 40 mW for the blue curves. With these pump levels, the systems were above threshold in all cases. As an example, the output power of the RL with 31 RDBG as a function of the pump power is shown in the inset of the figure. For the measurements we used a spectrum analyzer with a resolution of 0.01 nm.

One can see from Fig. 4 that, in general, the spectrum contains several peaks (spectral modes) in the range of interest; there are two peaks for the RL with 7 gratings and between five and seven for the case of the cavity with 20 gratings. For the laser with 7 gratings the two peaks maintain their positions and relative intensities as the pump power is increased. However, as the number of gratings in the the RL structure increases, the competition between modes induces strong fluctuations that depend on the pump power. One observes that the relative intensities of the peaks vary with the pump power, but that their spectral positions, indicated by the vertical lines, remain fixed. Concerning the spectral width of the lines, we observe that it appear to be fairly independent of the number of gratings (or at least there is no clear trend). In the inset of

#103290 - $15.00 USD Received 31 Oct 2008; revised 13 Dec 2008; accepted 13 Dec 2008; published 5 Jan 2009

Fig. 4 we present the total emitted power as a function of the pump power for the laser with 31 gratings. We observed that the threshold points are slightly different for each realization and decrease with the number of gratings in a fiber.

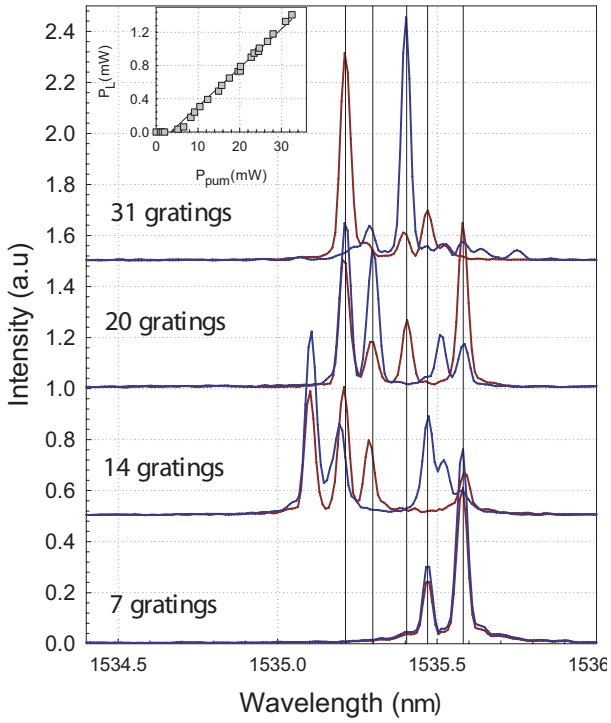


Fig. 4. Output spectra of the random lasers with 7, 14, 20 , and 31 of gratings, for two values of the pump power well above the lasing threshold; the red curve is for a pump of 20 mW, and the blue one for 40 mW . The vertical lines mark the spectral positions of the emission lines. The inset shows the total emitted power as a function of the pump power for the laser with 31 gratings.

For pump powers well above threshold, the emission spectra were not stable, even at a fixed pump power. In the enclosed movie, we present an example of the real-time temporal evolution of the output spectrum of the RL with 31 gratings and a pump power of 40 mW. One can see that there is a continuous shifting and interchange of power between the spectral modes during the 32 seconds that last the presentation. At some moments one of the lines dominates, while at others several lines have approximately the same intensity and, in some cases, some of the lines merge. Notice that the evaluation of each spectrum by the analyser takes about 1 second, which is much shorter than the evolution of the observed fluctuations.

## 3. Discussion

The propagation of light through our array of Bragg gratings is a particular case of the more general problem of wave propagation through 1D random media. An important feature of such a system is that it can have high transparency at some special (resonance) wavelengths [24], accompanied by the presence of ”hot spots” within the cavity. This effect can be observed in the localization regime; that is, when $L >> \xi$, where $L$ is the length of the system and $\xi$ is the

#103290 - $15.00 USD Received 31 Oct 2008; revised 13 Dec 2008; accepted 13 Dec 2008; published 5 Jan 2009

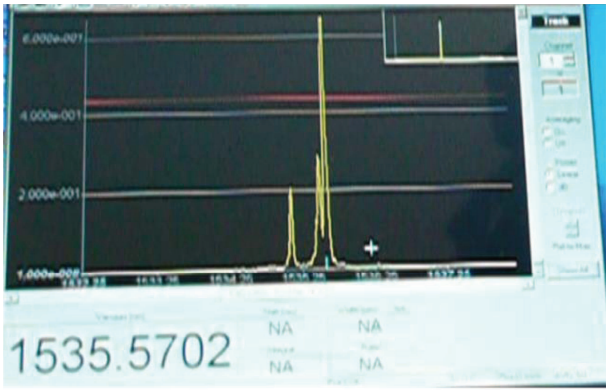


Fig. 5. An example of the temporal evolution of the output spectrum of the RL with 31 gratings (Media 1). The pump power is 40 mW. The instant spectral position of the strongest peak is shown in the bottom left corner.

localization length. The latter parameter can be estimated from the characteristic, exponential decay of the average transmission as a function of the length of the array. In particular, we estimate this quantity using the expression [25] $\langle \ln T \rangle / (2L) \propto -1/\xi$ and, for the RDBG used in our experiments, the localization length is found to be about 6 gratings. This quantity was found from calculations based on the transfer matrix method using parameters that correspond to those of the fabricated gratings. From the length (5 mm) and typical reflectivity ($R \approx 0.08$) of the fabricated gratings, which have a central wavelength $\lambda = 1535.5\,\mathrm{nm}$, we estimate that the average period of the grating is $\Lambda = 525.72\,\mathrm{nm}$, the number of periods is $N = 10^4$, and the modulation of the refractive index is $\delta n \approx 4 \times 10^{-5}$.

In Fig. 6 we present a color-level plot of the mean field intensity as a function of the wavelength and position along the RDBG calculated on the basis of transfer matrix approach for one particular realization of the disorder. Multiple scattering of light inside the random system results in the localization of light of some wavelengths, and in the formation of ”hot spots”, i.e. regions of high field intensity. Some of these features can be observed in Fig. 6. In such regions, the intensity of the light can be about six times higher than the intensity of the incident light. A simplified view of this complex system is obtained if one considers the two sets of random gratings, in front of and behind such a ”hot spot,” as a pair of ”effective” reflectors that form a Fabry-Perot cavity for this particular resonance wavelength.

In Fig. 7(a) we present the calculated spatial distributions of the intensities of the light for the four wavelengths indicated by arrows in Fig. 6. The field intensity that corresponds to the wavelength $\lambda_4$ decays exponentially along the RDBG and the transmittance of the system at this wavelength is exponentially small. The distributions that correspond to the wavelengths $\lambda_1$, $\lambda_2$ and $\lambda_3$ have maxima (”hot spots”) and the transmittance of the system at these wavelengths is close to unity. These distributions are associated with resonance modes. Notice that the half-width of the high intensity peaks or hot spots is about 3 gratings, which is consistent with the localization length obtained from the exponential decay of the mean transmission. This means that the spatial intensity distribution in the cavity has a width that is of the order of the localization length $\xi$ of the grating array and is located near the middle of the random system [11]. In the figure, there are two curves that correspond to the wavelength $\lambda_2$; the lower curve is for an array of $N = 27$ gratings, and the upper one is for an array of $N = 31$ gratings. One can see that the intensity inside the cavity grows with the increase of the length of the array, but its

#103290 - $15.00 USD Received 31 Oct 2008; revised 13 Dec 2008; accepted 13 Dec 2008; published 5 Jan 2009

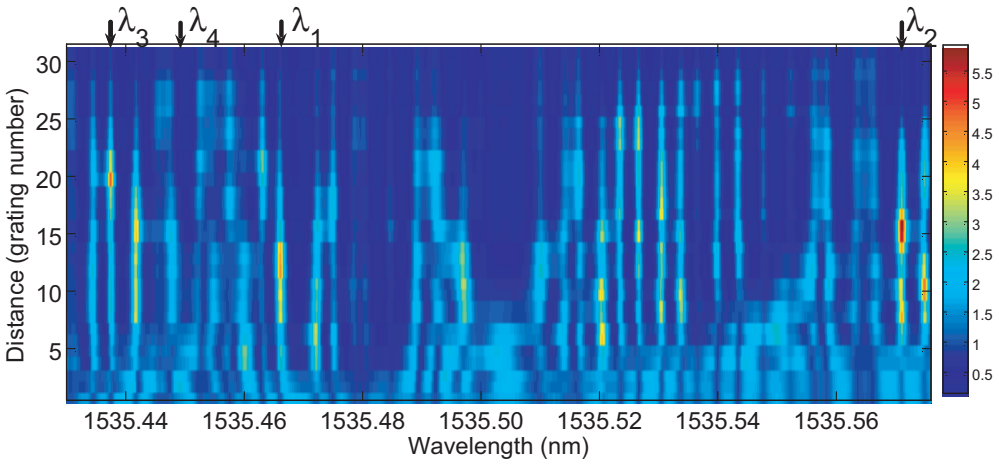


Fig. 6. Color-level plot of the light intensity in a random array of $N$ = 31 gratings, as a function of the wavelength and position along the array.

shape changes only slightly.

The dependence of the maximum intensity of the resonance modes at the wavelengths $\lambda_1$ (blue), $\lambda_2$ (black), and $\lambda_3$ (green) on the number of gratings is shown in Fig. 7(b). The gratings are sequentially added to the rear side of the array. One can see that the intensity of the light in the cavity grows with the addition of gratings and saturates when the the reflectivity of the "rear mirror" reaches its maximum value. Obviously, the reflectivity of the "front mirror" is not affected by the addition of gratings at the rear end of the system and, consequently, remains fixed.

Upon increasing the number of gratings, new resonant cavities can be formed near the middle of the complete system. The new resonance mode occurs at a wavelength that is different from that of the mode of the shorter array, but its Q factor is similar. The experimental observation that the resonance modes of the effective cavities formed in the shortest laser (with 7 gratings) are present in the lasing spectrum of the longest laser (with 31 gratings) can be understood in these terms.

The effective cavities have high quality factors and rather short lengths, of the order of the localization length. The typical FWHM of the spectral lines generated close to the threshold are about $0.02-0.04$ nm and, under our experimental conditions, we did not observe any narrowing of the lines with an increase in the pumping. The spectral width of the resonance mode can be evaluated from the solution of the dispersion relation for the modes of a cavity. The imaginary part of a complex frequency of the cavity mode is given by $\Delta\omega_c = c/(2n_{eff}a_c)\ln(R_f R_r)$, where $n_{eff}$ is the effective refractive index of the cavity, $a_c$ is the length of the cavity, and $R_{f,r}$ are the amplitudes of the reflection coefficients of the "front" and "rear" mirrors that form the cavity. Since the reflection amplitudes $R_f$ and $R_r$ are close to unity, we can expand the logarithm and obtain $\Delta\lambda_c = \pi\lambda^2/(a_c n_{eff})(T_f + T_r)$, where $T_{f,r}$ are the amplitudes of the transmission coefficients of the "front" and "rear" parts of the nontransparent regions, $T_{f,r} \approx \exp(-a_{f,r}/\xi)$, $a_{r,f}$ are the lengths of the corresponding nontransparent parts [26]. Since $a_c$ is of the order of localization length $\xi$, for the cavity formed in the middle of the grating array we obtain a $\Delta\lambda_c$ of about 0.029 nm. This agrees with the experimental estimation of this width. The effective cavity quality factor $Q = \lambda/\Delta\lambda_c$ can be estimated from the calculated and experimentally obtained spectral widths. We find that for our laser Q is about $5\times10^4$.

#103290 - $15.00 USD Received 31 Oct 2008; revised 13 Dec 2008; accepted 13 Dec 2008; published 5 Jan 2009

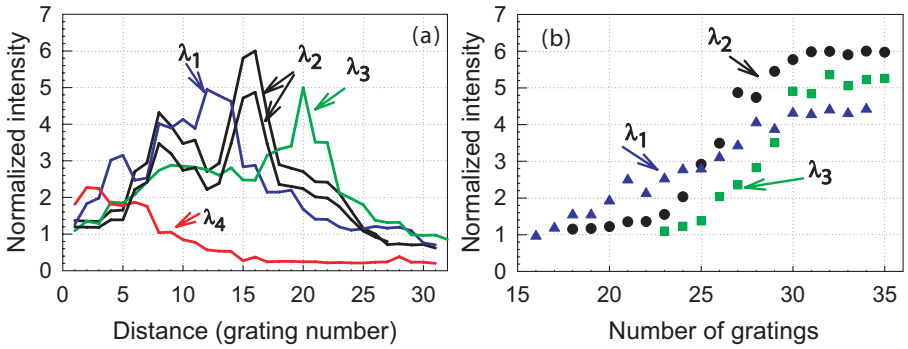


Fig. 7. (a) The spatial distribution of the intensity of the light inside the grating array for four different wavelengths marked in Fig.6. The two plots for the wavelength $\lambda_2$ correspond to the arrays with 31 (upper curve) and 27 gratings (lower curve). (b) The maximum intensity of the field in the effective cavity as a function of the number of gratings sequentially added to the rear side of the cavity. The data corresponds to the resonant modes that occur at the wavelengths $\lambda_1$ (blue), $\lambda_2$ (black), and $\lambda_3$ (green).

When optical gain is introduced into the random system, one can expect that the resonance mode with the largest Q factor starts to oscillate first. Since different cavities are localized in different regions of the fiber, and the pumping occurs from one of the end of the fiber and fills its whole length, the pump conditions of one cavity are unaffected by the other cavity. At higher pump powers, the lasing modes can shift away from the initial cavity resonance modes due to Kerr-type nonlinearities, the uneven distribution of intensity in the fiber, and locall saturation of the fiber gain. This induces the strong fluctuations observed in the lasing spectra shown in Figs. 4 and 5.

## 4. Summary and conclusions

We have implemented and studied a random 1D fiber laser. The laser consisted of an array of randomly distributed Bragg gratings recorded directly in an Er/ Ge co-doped single-mode fiber pumped at 980 nm. The output emission power of the system presents a clear lasing threshold behavior. Unlike other random lasers reported in the literature, the configuration under consideration does not have any resonance at the pumping wavelength, which permits efficient and spatially uniform pumping for all the longitudinal modes. The emission spectra of the random laser shows that at some pump levels there is a competition between several of the resonance longitudinal modes of the fiber laser random cavities, the number of which increases with the number of gratings. While the relative power of the emission spectral peaks varies among the different lines, the positions of the generated lines remain fixed. The nature of the fluctuations of the lines belonging to different cavities shows that the lengths of the cavities formed are close in their magnitudes, as are their Q factors. Even under fixed external conditions fluctuations in the output power with time were observed.

## Acknowledgments

The authors greatly appreciate the stimulation and support of Prof. A. A. Maradudin, and acknowledge fruitful discussions with Prof. V. Freilikher and Dr. S. Stepanov. This research was supported in part by CONACYT (México), under Grant 47700-F, and a grant from the University of California Institute for Mexico and the United States (UC MEXUS) and the Consejo

#103290 - $15.00 USD Received 31 Oct 2008; revised 13 Dec 2008; accepted 13 Dec 2008; published 5 Jan 2009

Nacional de Ciencia y Technologia de México (CONACYT), Award UCM-42127.

#103290 - $15.00 USD Received 31 Oct 2008; revised 13 Dec 2008; accepted 13 Dec 2008; published 5 Jan 2009